PHYSICAL REVIEW D **95,** 015027 (2017)

Faking ordinary photons by displaced dark photon decays

Yuhsin Tsai,[1] Lian-Tao Wang,[2,3] and Yue Zhao[4]

[1]*Maryland Center for Fundamental Physics, Department of Physics, University of Maryland, College Park, Maryland 20742, USA*

[2]*Department of Physics, The University of Chicago, Chicago, Illinois 60637, USA*

[3]*Enrico Fermi Institute and Kavli Institute for Cosmological Physics, The University of Chicago, Chicago, Illinois 60637, USA*

[4]*Michigan Center for Theoretical Physics, University of Michigan, Ann Arbor, Michigan 48109, USA*

(Received 27 September 2016; published 30 January 2017)

A light metastable dark photon decaying into a collimated electron/positron pair can fake a photon, either converted or unconverted, at the LHC. The detailed object identification relies on the specifics of the detector and strategies for the reconstruction. We study the fake rate based on the ATLAS (CMS) detector geometry and show that it can be O(1) with a generic choice of parameters. Especially, the probability of being registered as a photon is angular dependent. Such detector effects can induce bias to measurements on certain properties of new physics. In this paper, we consider the scenario where dark photons in final states are from a heavy resonance decay. Consequently, the detector effects can dramatically affect the results when determining the spin of a resonance. Further, if the decay products from the heavy resonance are one photon and one dark photon, which has a large probability to fake a diphoton event, the resonance is allowed to be a vector. Because of the difference in detectors, the cross sections measured in ATLAS and CMS do not necessarily match. Furthermore, if the diphoton signal is given by the dark photons, the standard model $Z\gamma$ and ZZ final states do not necessarily come with the $\gamma\gamma$ channel, which is a unique signature in our scenario. The issue studied here is relevant also for any future new physics searches with photon(s) in the final state. We discuss possible ways of distinguishing dark photon decay and a real photon in the future.

DOI: 10.1103/PhysRevD.95.015027

I. INTRODUCTION

The Large Hadron Collider (LHC) is currently the most energetic high energy facility running in the world. The center of mass energy of the proton-proton collision has reached 13 TeV, and it provides us direct probes to new physics beyond the standard model on the energy frontier. To extract information from each collision, final states are registered on detectors and further go through highly nontrivial object reconstruction procedures in order to be identified. Thus the conclusions one draws from the LHC highly depend on the object reconstruction strategies. It is interesting and important to investigate the possible loop holes in object identification procedures, which may lead us to a conclusion different from what really happened.

A photon is one of the most important objects from the collider physics point of view, especially on a proton-proton collider where dominant final states are QCD hadrons. In this paper, we focus on the possibilities of faking the photon signature by exotic hidden sector decays. The first possibility is to have two or more collimated photons in final states. Such collimated photons can be the decay products of a highly boosted light particle. A close analogy that happens in the Standard Model (SM) is the highly boosted pion decaying to two photons through the anomaly vertex. Such a channel has been checked carefully in the content of Higgs decay. Instead of a pion in SM, a light particle in the hidden sector, which is easily isolated with other particles in final states, can also decay to collimated photons. This possibility has been discussed in several places (e.g., [1–11]). It is also shown in several works [12,13] that making a highly boosted (so the two collimated photons are too close to be resolved) hidden scalar decay into two SM photons within the detector is challenging, and the charged particles that are introduced to decay the hidden scalar into SM photons can be highly constrained.

Another way of faking the photon signal, which we explore in this work, is through a displaced decay into charge leptons. If a light hidden sector particle decays to a pair of collimated electron and positron at a distance comparable to the detector size, such objects have a good chance to fail the lepton tagging and be identified as a photon at the LHC. Particularly, when a real photon interacts with materials and converts into an electron/positron pair, the photon gives the same final state particles as from the hidden sector decay. More interestingly, as we will show, due to the subtle object identification strategies in the detector, the angular distribution of the fake photon signal depends on the dark photon lifetime; i.e., the detector geometry can introduce a bias to signal angular distribution. Such a bias can be important in determining the property of new physics. For example, if one or more dark

photons are produced due to a heavy particle decay, studying the angular distribution of the signal events is the most common way to determine the spin of the resonance. However, the nontrivial angular distribution of the fake photon events can change the result in such an analysis and give a different result of the resonance spin.

In this paper, we focus on the scenario where a displaced dark photon decays as $\gamma' \to e^+e^-$. Some preliminary ideas about the photon faking from the dark photon decay is discussed in [13,14], which focused on the possibility that the decay of a dark photon only fakes a converted photon. In [14], it is suggested that if a photon signal really comes from a dark photon decay, one can distinguish it from the SM photon by checking whether the signal is more populated in the converted photon category.

However, we show in this paper that the above conclusion may not be complete. Through a more careful study of the photon identification criteria and detector geometry, we show the dark photon decay can also fake unconverted photon signals. Specifically, for some generic choices of parameters, the relative rates for dark photons to be tagged as converted versus unconverted photons can be similar to SM photons. Thus by simply checking the ratio of converted/unconverted photons in the signal region may not be enough to distinguish the two final states [15].

The outline of this paper is as follows. In Sec. II, we discuss the details on photon identification and show how a dark photon decaying at a different part of the detector can fake a photon, either converted or unconverted. In Sec. III, we classify the dark photon decay identification into four categories and study the probability of each category for generic choices of parameters. We estimate the ratio between the converted and unconverted photon events, which can be used to examine the fake photon signal. Also we compare the kinematics of the electron/positron from a dark photon decay to that from a photon conversion and show that they can be similar to each other. In Sec. IV, we consider a benchmark model where a heavy resonance decays to two dark photons or one SM photon plus one dark photon. We discuss several interesting model building subtleties in these cases. In Sec. V, we carry out a detailed study on dark photon parameter space and show that a generic choice of dark photon mass and mixing can easily give a signal rate in a diphoton search to be comparable to the SM background. Thus the fake photon signal is important to be taken into consideration in certain photon-related measurements. We also present the distortion of angular distributions after taking into account the detector effects. Several new physics searches, such as lepton jet searches and a monophoton search, may be applied to constrain our parameter space. We find our scenario can easily be consistent with these searches. At last in Sec. VI, we summarize and discuss the possible ways to distinguish our scenario from the conventional ones.

II. PHOTON SELECTION CRITERIA

When a highly boosted and metastable particle decays to a collimated e^+e^- in the tracker, there is a good chance for the object to be identified as a photon. To estimate the probability of registering the metastable light particle decay as a photon, we first discuss the criteria on the photon identification at both ATLAS and CMS.

We note that there can be several differences between the fake and real converted photons. First, the two leptons from a dark photon decay can have a different energy distribution from the one from a photon conversion. Moreover, the probability of a dark photon being registered as a converted/unconverted photon depends on its lifetime, which can be different from the conversion rate of SM photons. The detailed location of photon conversion should also follow the distribution of the material, while the dark photon decay is not bonded to this. To observe the differences, we need either a large number of signal events or a more careful study of the converted e^+e^- kinematics as we will discuss in the later sections.

Whether the dark photon decay is identified as a photon and whether it fakes a converted or unconverted photon all depend on the decay location and the angle between the electron and positron in the final state. Taking these into account, we investigate the possibility of obtaining a sizable photon faking probability that satisfies existing bounds on the various displaced signals. Our discussion will mainly be based on the details of the ATLAS detector [19,20]. The tracker at CMS has a similar geometry to that at ATLAS, but the angular resolution of the electromagnetic calorimeter (ECAL) in the (η, ϕ) direction is worse in distinguishing the columnated e^+e^- from a single photon. Therefore, the probability for a dark photon to fake a SM photon at CMS is likely to be higher than that at ATLAS. We discuss more details of the CMS detector later in this section.

A converted photon is a cluster of energy deposition in the ECAL associated with one or two tracks that appear in the middle of the tracker. More precisely, the reconstructed track should start after the first layer of the tracker, which is about 34 mm away from the central axis of the detector in the barrel region. The number of tracks can be either one or two depending on whether the photon conversion is symmetric or asymmetric. Furthermore, to seed the track, there need to be at least three space points in either the pixel or the semiconductor tracker (SCT) [21]. Thus any electron/positron that appears after the third-to-the-last layer of the SCT (it is about 371 mm away from the central axis in the barrel region) will not leave a reconstructible track. We emphasize that a converted photon cannot have a track that registers a hit at the first layer of the pixel in the tracker. This is because the conversion can happen only in places with materials. Thus for a metastable particle, if its decay happens between the first layer of the pixel and the third-to-the-last layer of SCT, it will be identified as a converted

photon. The converted photon can in principle be constructed in the transition radiation tracker (TRT), but the reconstruction efficiency is expected to be much lower for high energy photons. Different from the clear tracks obtained in the pixel and SCT, which allow the photon reconstruction using a single electron (asymmetric conversion), the standard TRT tracks are much less reliable and need both of the tracks to identify a converted photon. If the photon p_T is too large, the electron and positron are hardly separated in the TRT. This is why the 20 GeV converted photon has a much lower efficiency than the one of the 5 GeV photon, as is shown in Fig. 6 of [18]. Hard p_T cuts are usually imposed in a typical diphoton resonance search. For instance, the leading photon needs to have $p_T \gtrsim 100$ GeV in [22,23], and it is very unlikely that a converted photon can be constructed by hits at the TRT.

It is a little bit subtle if the metastable particle decays after the third-to-the-last layer of the SCT. If the decay happens before the first layer of the ECAL, which is about 1500 mm away, there are no tracks associated with the energy deposition in the ECAL. What kind of object the decay signal will be identified as depends on the separation between electron/position when they hit the ECAL.

The first layer of the ECAL in ATLAS has extremely good resolution on pseudorapidity η, $\Delta\eta \sim O(10^{-3})$. If the η separation of energy deposition from electron/position cannot be resolved, such an event will be identified as a normal photon. If the separation can be resolved, the signal structure is similar to the one from a neutral pion decaying into two photons. Such an object will not be identified as a single photon. If the separation is very large, so that the energy deposition is grouped as two clusters in the ECAL, the final state is identified as two photons close to each other. The last possibility is very unlikely to happen in our scenario since we assume the metastable particle is very light and thus highly boosted, so we will not consider this possibility in the later discussion.

The precise angular cut at the first layer of the ECAL, which determines if the signal is a single photon or not, is complicated and η dependent. To proceed, we make a rather conservative assumption to simplify the calculation by requiring the separation Δx in length in the first layer of the ECAL to be within the average width of the strip cells ($\Delta x < 4.7$ mm). The bound is similar to the one discussed in [12], which uses the argument that a π^0 with 65 GeV energy can be distinguished from a photon in Higgs searches. There is one subtle difference, however, between the two assumptions. The π^0 decays promptly in the detector, while our metastable particle needs to decay after the third-to-the-last layer of SCT. The spatial separation from the hidden particle decay is smaller than that of the π^0 decay if they share the same opening angle.

In the CMS detector, angular resolution of the lead tungstate crystals in the ECAL is $\Delta\eta \sim O(10^{-2})$, and a dark photon decay that passes the angular cut at ATLAS can also look like a single photon in the CMS. To identify the converted photon, the converted safe electron veto used in the CMS also removes tracks with a hit in the innermost tracker layers [24]. The first layer is about 44 mm away from the beam pipe, which is similar to the 34 mm in the ATLAS setup for our purpose. The crystal calorimeter takes signals up to 1.79 m, which is not too far from the requirement at ATLAS of having the ECAL signal before 1.5 m. Thus the faking rate for a metastable dark photon decay can be comparable to each other in two experiments, with only mild differences.

At last, let us discuss more details about the possibility that the dark photon decays either before the tracker or after the first layer of the ECAL. If the decay happens before the tracker, the object will not be identified as a converted photon since the reconstructed tracks have hits on the first layer of the pixel. In this case, a search of the prompt lepton jets [25] can be useful in constraining the scenario, as we will study in Sec. V. If the decay happens after the first layer of the ECAL ($1590 < r$ mm in ATLAS), there is a large chance that such a decay will not be constructed as a well-defined object [26]. In this case, since the search of the monophoton in ATLAS [28] defines the missing transverse energy (MET) to be the imbalance of the total momentum of the well-constructed objects, the resonance decay into two dark photons—where one has later decay after the ECAL and one is inside the tracker—may be considered as a monophoton signal. We study the bound in Sec. V under this conservative assumption. Further, there are specially designed searches if the decay happens inside the hadron calorimeter (HCAL, > 1970 mm in ATLAS); for example, displaced lepton signals at the HCAL can be applied [29,30]. However, because of the strong requirements on event selection, especially requiring that both metastable particles decay in HCAL, these searches constrain only 8 TeV dark photon pair production at the picobarn level. This is a much weaker constraint compared to the monophoton search.

III. OBJECT IDENTIFICATION SUMMARY

Here we summarize the object identification criteria used in this work. As we discussed above, whether the dark photon decay is identified as a photon, especially whether it is a converted or unconverted photon, highly relies on the details of the detector. A precise simulation of the detector response is beyond the scope of this paper. Here we carry out a simplified procedure to estimate how the lifetime of metastable particles affect the object identification.

We classify the metastable particle decay into four regions:

Before tracker: If the decay happens before the first layer of the tracker, i.e. with a distance $\gtrsim$34 mm in ATLAS, the electron/positron can be identified, and the signal is not identified as a photon. The nonisolated leptons from a highly boosted light particle decay [with a boost factor $\sim\mathcal{O}(10^3)$] can be studied in the lepton-jet search, and we

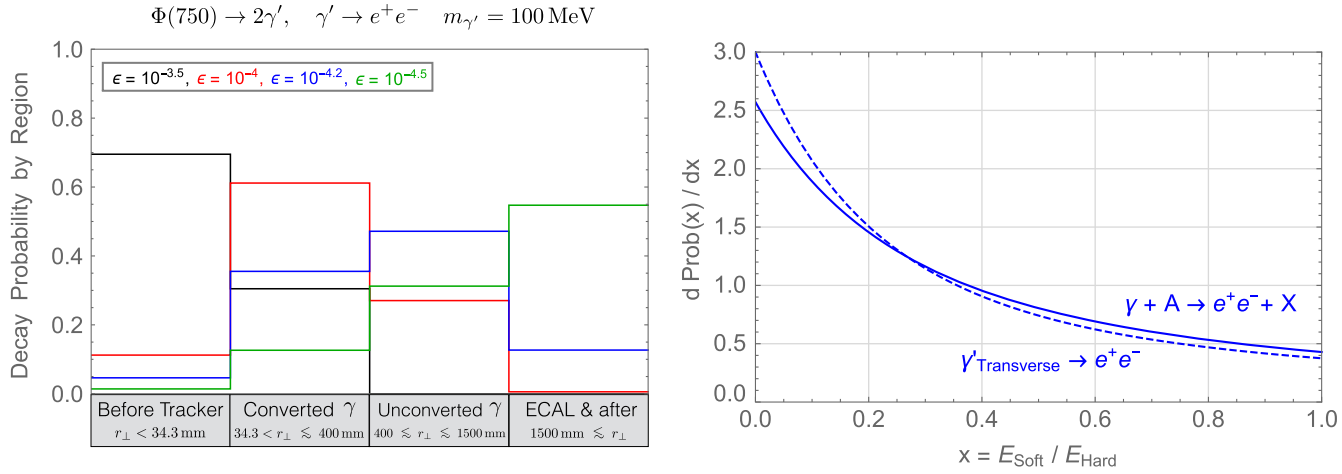

FIG. 1. Left: Probability of one dark photon decay by regions, where $r_\perp$ is the transverse distance of the decay vertex from the beam pipe. We take the detailed positions of the third-to-the-last layer of SCT from [19] in our analysis. The probability for each region is η dependent, and we integrate the result from the central region to $|\eta| = 2.3$ in our estimation based on our simulation. Right: Comparison of energy ratios between the hard and soft leptons from the SM photon conversion and the dark photon decay. The plot is made by assuming $m_{\gamma'} = 100$ MeV, and the decay into e^+e^- is from the transverse mode of γ'. When $m_{\gamma'} \ll E_{\gamma'}$, the distribution is insensitive to the size of $m_{\gamma'}$.

will show in Sec. V how the existing search constrains the parameter space.

Converted γ region: If the decay happens within the tracker and can leave at least three space points in either pixel or SCT, we identify such a decay as a converted photon. The details on the ATLAS detector are taken from [19]. We emphasize that this is an oversimplified criterion for identifying converted photons, and having at least three space points in the pixel or the SCT is only a minimal requirement to seed a track. In a more complete search, there can be additional procedures on the track reconstruction.

Unconverted γ region: If the decay happens before the ECAL and after the tracker region so that there are no more than three layers of the SCT to be available to reconstruct the track, we identify the decay signal to be an unconverted photon. This is under the assumption that the open angle between electron/position from the metastable particle decay is too small to be resolved as two photons in the ECAL. We will see in the later discussion that the angular cut can be satisfied in the model we are interested in.

ECAL and after: If the decay happens within or after the ECAL, we do not identify such an object as a photon. How it will be identified depends on where the decay happens. It is possible that such a late decay of dark photons will be treated as missing energy. If one of the decay products from the heavy resonance is identified as a photon, while the other one is registered as MET, the monophoton search can be used to constrain the parameter space. We will present this constraint in Sec. V.

In our discussion we focus on the model with $2m_e < m'_\gamma < 2m_\mu$, where a dark photon preferentially decays into e^+e^-. This decay is induced by the kinetic mixing between the SM photon and an extra $U(1)'$ gauge boson, i.e., $\mathcal{L} \supset (\epsilon/2)F_{\mu\nu}F'^{\mu\nu}$. The dark photon, defined in the mass basis after canonical normalization, has a proper decay length

$$c\tau_{\gamma' \to e^+e^-} \simeq \left(\frac{\epsilon^2 \alpha_{\mathrm{EM}} m_{\gamma'}}{3}\right)^{-1} = 8 \times 10^{-3}\ \mathrm{cm} \left(\frac{10^{-4}}{\epsilon}\right)^2 \left(\frac{100\ \mathrm{MeV}}{m_{\gamma'}}\right). \quad (1)$$

To illustrate the idea with some concrete results, we take the 750 GeV resonance [22,23,31,32], which has drawn a lot of attention previously, as an example in the collider study. However, we emphasize that the discussions in this work can be applied for many photon-related searches at the LHC. In Fig. 1 (left), we present our simulation results on the probability of having dark photons with different lifetimes decay in the four regions discussed above. The plot assumes the dark photon, which carries a mass $m_{\gamma'} \sim 100$ MeV, is generated from the decay of a 750 GeV scalar resonance produced by the gluon fusion. If the heavy resonance is produced by $q - \overline{q}$ scattering, it may have a different boost along the beam direction due to different parton distribution functions of $q\overline{q}$ and gluon. This can affect the angular distribution of the final states in the lab frame, and detector effects can cause a subtlety. We study both cases and find a negligible difference between the two scenarios.

This result takes into account the geometry of the ATLAS detector at different η angles. In principle, one can study whether there are fake photons from the dark photon decays by calculating the ratio of the numbers of the converted versus unconverted photons. Depending on the

statistics of photon signals, we can constrain the decay lifetime by requiring this ratio to be compatible with the one from real photon events. As is shown in Fig. 1 (left), this can be satisfied when the kinetic mixing $\epsilon \sim 10^{-4}$, which is also consistent with current constraints from various dark photon searches. As an example, we take as a benchmark point, i.e., the diphoton resonance search at around 750 GeV, that the current statistics in the high invariant mass region is not good enough to impose a strong constraint on ϵ by checking the converted/unconverted ratio. Thus there is still a generic choice in our parameter space so that this ratio is compatible with that of a real photon. However, one expects that this can be reasonably improved in the future when having a higher statistics.

One may suggest to distinguish converted photon and light dark photon decay by comparing the energy ratio between e^+e^-. However, we show in the right panel of Fig. 1, if the dark photon from the 750 GeV heavy resonance decay is dominantly in transverse modes [33], the asymmetry of the two leptons from $\gamma' \to e^+e^-$ is similar to that in the converted photon process $\gamma + A \to e^+e^- + Z$, where A and Z stand for the initial and final states of material that assists the conversion. This is because the electron from a transversely produced dark photon decay tends to be parallel or antiparallel to the dark photon spin; boosting γ' into the lab frame makes one lepton harder than the other one, which generates the asymmetry [34].

Besides distinguishing photons in the inner detector, we may use the showering shape in the ECAL to tell the difference between a single photon and a highly boosted γ' decay into e^+e^-. The "photon jet" objects have been studied for the Higgs search [8], although the focus is on a (pseudo)scalar particle decaying into two photons. Since the dark photon decay usually deposits most of the photon energy into one of the leptons, the ECAL signal may better resemble a single object. A more detailed study, including the detector response of the electron signal, is necessary to identify the dark photon decay.

Another way to distinguish the dark and SM photons is to study the conversion rate of the photon events. For SM photons, the ratio $R \equiv N^{\gamma}_{\rm cv}/N^{\gamma}_{\rm uc}$ between the number of converted $N^{\gamma}_{\rm cv}$ and unconverted $N^{\gamma}_{\rm uc}$ events is about 0.25 when the photon rapidity $|\eta| < 1.5$ [35]. In Fig. 2, we compare this ratio to the dark photon events with the event number being equal to the total number of signals $N^{\gamma'}_{\rm sg}$ times the probability $P_{\rm cv}$ or $P_{\rm uc}$ of the dark photon being identified as a converted or unconverted photon, i.e., $N^{\gamma'}_{\rm cv/uc} = P_{\rm cv/uc}N^{\gamma'}_{\rm sg}$. The ratio $R_{\gamma'+\gamma} = (P_{\rm cv}N^{\gamma'}_{\rm sg} + N^{\gamma}_{\rm cv})/(P_{\rm uc}N^{\gamma'}_{\rm sg} + N^{\gamma}_{\rm uc})$ is shown in the blue curve in Fig. 2, which represents the converted versus unconverted photon ratio without the presence of the other SM background. When the kinetic mixing parameter satisfies $\epsilon \lesssim 10^{-4.6}$, the photon decay length is comparable to the size of the detector, the asymptotic value of the ratio for an even

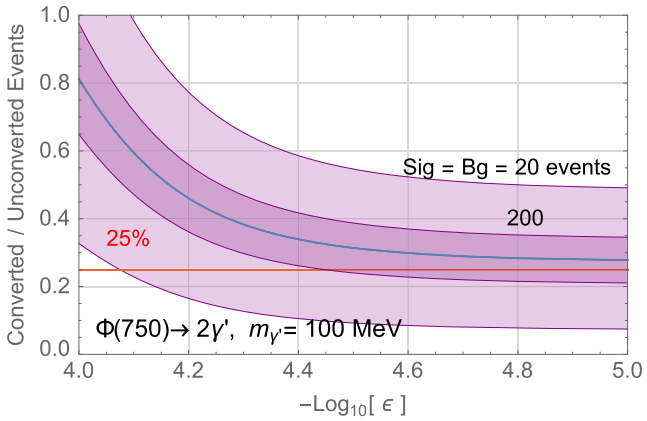

FIG. 2. Ratio of the fake photon events being identified as converted and unconverted photons. The blue curve is derived from the ratio of the dark photon decay probability in the converted and unconverted regions. The light (dark) purple band includes a 2σ fluctuation of the photon events as in Eq. (2) assuming 20 (200) events of both the signal and the background. According to [35], we take the ratio of converted versus unconverted photon events in the SM to be 25%.

smaller ϵ is determined by the geometry of the detector. To include fluctuation of the signal and background, we show a colored band of the event ratio with the upper and lower boundaries, which corresponds to a 1.64σ uncertainty that is comparable to the 90% C.L. deviation from the expected ratio

$$R^{\pm}_{\gamma'+\gamma} \equiv \frac{N^{\gamma'+\gamma}_{\rm cv}}{N^{\gamma'+\gamma}_{\rm uc}}\left(1 \pm 1.64\sqrt{(N^{\gamma'+\gamma}_{\rm cv})^{-1} + (N^{\gamma'+\gamma}_{\rm uc})^{-1}}\right). \quad (2)$$

Here $N^{\gamma'+\gamma}_{\rm cv} = P_{\rm cv}N^{\gamma'}_{\rm sg} + 0.2N^{\gamma}_{\rm bg}$, and $N^{\gamma'+\gamma}_{\rm uc} = P_{\rm uc}N^{\gamma'}_{\rm sg} + 0.8N^{\gamma}_{\rm bg}$. To illustrate the idea, we assume the production of fake photon events is of a femtobarn level, and the number of fake photon events is comparable to the SM photon background to play an important role. In Fig. 2, the light purple region assumes $N^{\gamma'}_{\rm sg} = N^{\gamma}_{\rm bg} = 20$, which gives an idea of the $R_{\gamma'+\gamma}$ deviation at the early 13 TeV run at the LHC. In this case, checking the ratio does not distinguish the two different photons when $\epsilon \lesssim 10^{-4}$. A stronger result can be obtained when $N^{\gamma'}_{\rm sg} = N^{\gamma}_{\rm bg} = 200$ with $\mathcal{O}(100)$ fb of data.

In the left panel of Fig. 3, we show the efficiency of a dark photon decay in the unconverted photon region that passes the open angle cut, assuming $\eta(\gamma') = 0$ for simplicity. The cut requires the e^+e^- pair that fakes a normal photon to hit the first layer of the ATLAS ECAL within a separation [36] $\Delta x < 4.7$ mm in the η direction, so the signal can be identified as a single photon. This is a rather conservative assumption compared to the estimation using boosted pions from the Higgs decay measurement [12]. These criteria are easier to be satisfied for a γ' with a larger

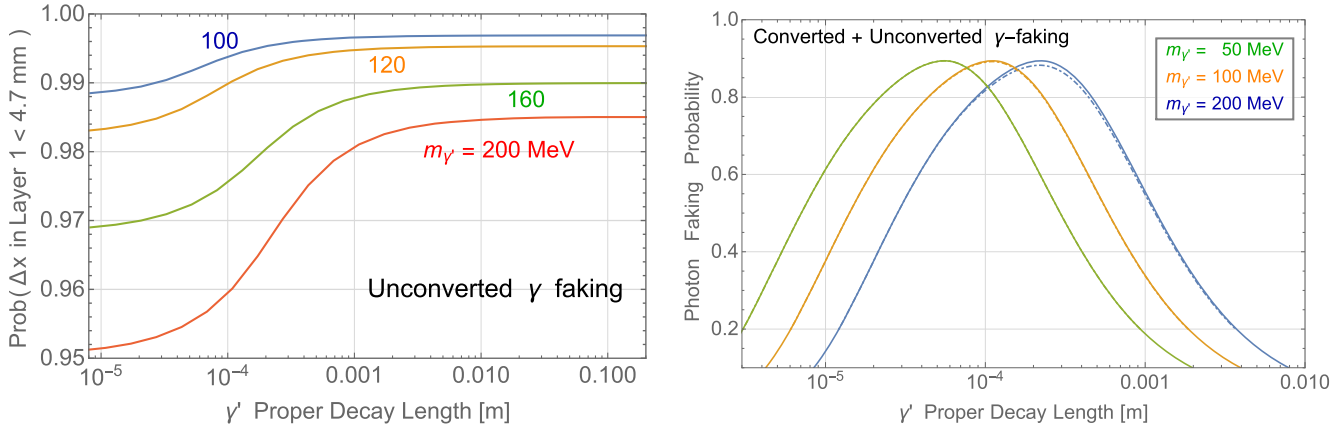

FIG. 3. Left: Probability of a dark photon produced from $\Phi(750) \to 2\gamma'$ decaying into e^+e^- between radial distance [371, 1500] mm (from the second layer of SCT to ECAL with $\eta = 0$) that has its two hits in the η direction of the strip cells (defined as Δx) to be within the average thickness of the cell (< 4.7 mm). Here we assume the γ' moves in the radial ($\eta = 0$) direction. Right: Probability of one dark photon fakes a real photon. The result is derived according to the decay probability with (solid curve) and without (dash-dotted curve) the upper bound on the angular separation in the ECAL for the fake normal photon signals. See Sec. II for more discussions. Here we estimate the acceptance of this cut by assuming dark photons to be produced in the transverse mode. After boosting the open angle to the lab frame, we calculate the acceptance as a function of the decay position.

boost (smaller $m_{\gamma'}$) or a longer decay length. This is simply because for a fixed value of Δx, a larger open angle between $e+/e-$ is allowed if the decay happens closer to the ECAL.

In the right panel of Fig. 3, we show the probability of a dark photon decay being identified as a photon in the ATLAS detector. The estimation is based on the probability of dark photon decaying in the converted and unconverted photon regions (solid curves). The dash-dotted curves in Fig. 3 contain the angular cut discussed above. As we can see in the plot, the difference between the probability with (solid curve) and without (dot-dashed curve) the angular cut is not significant. This is because an O(100) MeV dark photon is highly boosted from the decay of a 750 GeV resonance.

IV. MODELS

As illustrated in the sections above, we show how a dark photon can fake a SM photon. In this section, we establish how a dark photon can affect our understanding to underline physics from the model building point of view. Since a SM photon and a dark photon are not trivial to be distinguished with the current photon identification strategy, we emphasize that wrong conclusions that may be drawn without this subtlety in mind. To make the physics as clear as possible, we consider the simplest scenario where a heavy resonance is produced at the LHC and further decays to two dark photons or one dark photon and one SM photon. With the current photon identification, such a scenario can show up as a diphoton resonance. To be noted, such a benchmark scenario was originally motivated by the 750 GeV diphoton excess announced by ATLAS and CMS at the end of 2015. Although this excess has gone away in the new set of data, our work remains valid and meaningful since we are focused on the subtleties of object identification at the LHC and our study can be generically applied to any scenarios with a photon involved.

First, a heavy resonance decaying to two photons can be introduced by integrating out charged particles which couple to the heavy resonance. Since the electromagnetic coupling constant has been fixed, the signal rate is directly related to the mass of the charged particles as well as their coupling to the heavy resonance. Assuming the number of species and the electric charge of charged particles are not too large, one can derive an upper limit to the signal rate for such a diphoton channel by requiring perturbativity. On the other hand, if one or both photons are actually dark photons, the upper bound can be largely relaxed due to an undetermined dark photon coupling constant.

Further, the SM photon and Z boson are mixtures of $SU(2)_W$ and $U(1)_Y$ gauge bosons. If a heavy particle can decay to the SM photon, then very likely, there are channels with the Z boson in final states. Although the detailed numbers on relative decay branching ratios depend on the representations of particles running in the loop, one generically expects them to be O(1). However, if the heavy resonance only decays to two dark photons that fake the photon at the LHC, then the decay channels with the Z boson involved do not necessarily exist.

It is well known that a heavy vector boson cannot decay to two on-shell photons, thanks to the Landau-Yang theorem. If a heavy resonance is found in the diphoton channel, one naively eliminates the possibility that such a heavy resonance is a spin-1 particle. On the other hand, a heavy vector boson can decay to a SM photon and a dark photon, since the final states are not identical particles. Without understanding the fact that a dark photon can

easily fake a SM photon at the LHC, one can simply miss this possibility, which leads to confusion.

In the following discussions in this section, we discuss more details of this benchmark model. As stated previously, our paper was originally motivated by the 750 GeV diphoton excess, we choose our benchmark point where the resonance is 750 GeV, and we assume the diphoton channel signal rate to be 5 fb at 13 TeV. However, our conclusion and the physics we discuss do not rely on this excess at all.

A. Spin-0 resonance

Depending on whether the scalar resonance Φ is a real scalar or a pseudoscalar, similar to the dilaton or the axion Lagrangian, it can decay into dark photons through an operator,

$$\mathcal{L}_{\gamma\gamma} \supset \frac{g_d^2 y_\Phi}{16\pi^2 M_1'} \Phi F'^{\mu\nu} F'_{\mu\nu} \quad \text{or} \quad \frac{g_d^2 y_\Phi}{16\pi^2 M_2'} \Phi F'^{\mu\nu} \tilde{F}'_{\mu\nu}. \tag{3}$$

Such operators can be introduced by integrating out particles charged under a dark $\mathrm{U}(1)'$, where g_d is the $\mathrm{U}(1)'$ gauge coupling. Φ can be either a real scalar or a pseudoscalar. It is also possible that one of the decay products is a SM photon, so the possible decay channels are

$$\Phi(750) \to \gamma'\gamma', \qquad \Phi(750) \to \gamma\gamma'. \tag{4}$$

The latter decay, however, may require the existence of a light SM charged mediator. Actually, in this case, there should be a $\gamma\gamma$ mode as well. This can be parametrically suppressed by choosing $e/g_d < 1$. But then the $\gamma'\gamma$ mode is also suppressed relative to the $\gamma'\gamma'$ mode.

A scalar resonance can be produced through the gluon fusion, $q - \overline{q}$ scattering, or electroweak vector boson fusion (VBF). For the VBF process, the signal usually comes with forward jets and is relatively easy to be tagged on. Further, if the scalar can directly couple to W or Z bosons at tree level, it has to be a condensed field that charged under the SM electroweak gauge groups. Such a scenario can be highly constrained, and we do not consider the VBF production in the rest of the discussion.

If the heavy resonance couples to gluons through loop diagrams, its effective coupling can be characterized as

$$\mathcal{L}_{gg} \supset \frac{g_3^2 y_\Phi}{16\pi^2 M_1} \Phi \mathrm{Tr}[G^{\mu\nu} G_{\mu\nu}] \quad \text{or} \quad \frac{g_3^2 y_\Phi}{16\pi^2 M_2} \Phi \mathrm{Tr}[G^{\mu\nu} \tilde{G}_{\mu\nu}], \tag{5}$$

depending on whether Φ is a real or pseudoreal scalar boson. We will assume the diphoton rate to be 5 fb at 13 TeV. To obtain a 20 fb $\Phi(750)$ production with $\mathrm{Br}(\Phi \to 2\gamma') = 0.25$, we need a SM colored mediator carrying a mass $M_{1,2} \simeq 3$ TeV, and a $\mathrm{U}(1)'$ charged mediator with mass $M'_{1,2} \simeq N_F g_d^2 \times 1.5$ TeV. Here (N_F, g_d) are the flavor and $\mathrm{U}(1)'$ coupling of the mediator.

The Φ can also couple to $q - \overline{q}$, e.g., by sharing the same $SU(2)_L$ and $\mathrm{U}(1)_Y$ charges as the Higgs boson. If Φ is inert, so it does not condense or mix with SM Higgs, the Higgs measurement constraints can be avoided. The decay into dark photons is also not suppressed by the tree-level process into W/Z. In four component notation after electroweak symmetry breaking, the coupling can be written as

$$\mathcal{L}_{qq} \supset y_\Phi \Phi \overline{q} q \quad \text{or} \quad i y_\Phi \Phi \overline{q} \gamma_5 q. \tag{6}$$

However, one has to tune the flavor structure in order to obtain a large enough production while avoiding flavor constraints. If one assumes a flavor diagonal Yukawa coupling with a universal coupling for all light quarks, having a 20 fb production and $\mathrm{Br}(\Phi \to 2\gamma') = 0.25$ requires $M'_{1,2} \simeq N_F g_d^2 \times 0.7$ TeV.

B. Spin-1 resonance

If we allow a dark photon in the final states, it is also possible for the heavy resonance to be a vector boson, i.e., V_H^μ as a gauge boson of a condensed $\mathrm{U}(1)_H$. The Landau-Yang theorem forbids the massive vector decaying to two photons. It is possible that the heavy vector decays to two dark photons because they are not massless [5,37]. However, the decay rates are expected to be highly suppressed due to the small mass of the dark photon. On the other hand, it is possible that the heavy vector decays to one SM photon and one dark photon,

$$V(750) \to \gamma\gamma'. \tag{7}$$

In this case, the two particles in the final states are not identical; thus no more suppression is applied to this decay channel. The decay of the heavy vector boson can be characterized by effective operators, for example,

$$\mathcal{L}_{V_H} \supset \frac{e g_d g_H}{16\pi^2 \tilde{M}_1^2} F^{\mu\nu}_{V_H} F^\alpha_\nu F'_{\alpha\mu}, \tag{8}$$

where g_d and g_H are γ' and V_H gauge couplings of the heavy mediator running in the loop. Having a SM photon in the final state requires the existence of SM charged mediators. Since V_H is a color singlet, it cannot be produced through gluon fusion due to the Landau-Yang theorem. For a $q - \overline{q}$ production of V_H, the gauge coupling as large as $\sim 10^{-2}$ can give an $\mathcal{O}(10)$ fb production of V_H at 13 TeV. To obtain a sizable branching ratio, we need the mass of the SM charged mediator to be $\tilde{M} \sim \sqrt{g_d g_H N_F} \times 220$ GeV, where N_F is the number of flavors running in the loop.

Besides the loop-induced decay into (dark) photons, if the dark Higgs that gives the mass to the dark photon is also

charged under $U(1)_H$, V_H can decay into the dark Higgs and the longitudinal mode of the dark photon. Generically, the dark Higgs has a mass close to the dark photon; thus it is kinematically allowed for this dark Higgs to decay into two dark photons, and this decay can happen at the detector scale. When the decay of the dark Higgs happens inside the region of the unconverted photon identification, i.e., Region III from Sec. III, there is a chance that such a process can fake a SM photon. Since the typical separation between the four leptons is $\Delta R \sim m_{\phi_d}/2m_{V_H} \sim 10^{-4}$ for $m_{\phi_d} = \mathcal{O}(100)$ MeV, the four leptons from the decay can be within the angular resolution of the ECAL. The benefit of this scenario is that the heavy vector resonance decays through a marginal operator and no light charged particles at O(100) GeV need to be introduced to UV to complete an irrelevant operator. However, the detector study of such a scenario is more complicated, and we leave the detailed study of the reconstruction efficiency for future work.

C. Resonance as a heavy bound state

As we have seen in the previous discussion, if the heavy resonance decays through loop-induced irrelevant operators, a low suppression scale is usually needed in order to achieve a sizable branching ratio to signal channel. Another interesting possibility is that the heavy resonance is actually a bound state formed by a pair of new particles. If the new particle has a strong coupling to a light dark photon, there is a high probability that the bound state is produced instead of two free particles [38]. The bound state can be either a scalar or a vector. If it is a scalar, the annihilation decay is dominant by a pair of the force mediator, i.e., the dark photon. The decay width of the bound state can be estimated as

$$\Gamma \sim \frac{\alpha_{\gamma'}^5}{4} M_B, \tag{9}$$

where $\alpha_{\gamma'}$ is the dark photon coupling constant and M_B is the bound state mass. Three powers of $\alpha_{\gamma'}$ in Eq. (9) come from the wave function suppression in the bound state. It appears in all annihilation decay channels. Thus the dark photon pair decay channel is preferred for scalar resonance due to the strong coupling of the dark photon. On the other hand, if the resonance is a vector state, the $\gamma + \gamma'$ final state is preferred.

When the heavy resonance is a vector field, one interesting possibility is that the decay $V(750) \to 3\gamma'$ is comparable to the $\gamma\gamma'$ channel. Although the Landau-Yang theorem forbids the vector to decay into two SM photons, and the two dark photon channel is highly suppressed by a power law of $m_{\gamma'}$ over the resonance mass, there is nothing preventing the heavy resonance from decaying into three dark photons (see also [37]). When the dark photon has a much stronger coupling than that of the normal photon, the $3\gamma'$ channel may have a similar decay branching ratio to $\gamma\gamma'$, and the search of three photon resonance can be important. For example, as we discussed previously, the heavy resonance may be a vector bound state formed by the dark photon exchange. In this case, the dark photon needs to have a large coupling, such as $\alpha_{\gamma'} \sim 0.3$, in order to have a sizable probability to form a bound state at the LHC. If both decay processes are allowed, the decay branching ratios into $3\gamma'$ and $\gamma\gamma'$ are compatible,

$$\frac{\Gamma_{V_H \to 3\gamma'}}{\Gamma_{V_H \to \gamma+\gamma'}} \sim \frac{\alpha_{\gamma'}}{4\pi}\frac{\alpha_{\gamma'}}{\alpha} \simeq \left(\frac{\alpha_{\gamma'}}{0.3}\right)^2, \tag{10}$$

and the dark photons in the final states will further decay into collimated e^+e^- that can fake the SM photons. Searching for a resonance in 3-photon final states may provide an interesting probe to this possibility. On the other hand, the boost factor of the dark photon from 3-body decay is smaller than that from 2-body decay. Thus the dark photon will have a shorter decay length in the lab frame. This may change the efficiency of being identified as a photon, and a detailed simulation is necessary to take into account the detector effects.

V. SIMULATION RESULTS

Let us first focus on the scenario where the resonance is a scalar boson. There is a generic choice of parameter space, i.e., $(m_{\gamma'}, \epsilon)$, for a dark photon to fake a SM photon with a probability $\gtrsim 80\%$. To estimate the probability, we first simulate a parton-level process $gg \to \Phi(750) \to 2\gamma'$ using MadGraph5.2 [41] and the effective coupling in Eq. (3) coded using FeynRules 2.3 [42]. We carry out our analysis at parton level, and we do not expect the conclusion to change much after detailed detector simulations are included. We apply kinematic cuts $p_T(\gamma') > 300$ GeV ($0.4m_{\gamma\gamma}$ taken in [31]), $|\eta(\gamma')| < 2.37$ in event selections. For each dark photon, we take its $(E_{\gamma'}, \eta_{\gamma'})$ and calculate the corresponding decay probability in each photon identification region, as described in Sec. III. We carry out similar analysis for $q\bar{q} \to V(750) \to \gamma\gamma'$ as well. The energy calibrations on converted and unconverted photons are both small, i.e., $|E/E_{\text{true}} - 1| \lesssim 0.5\%$ from the ATLAS study [43], and we do not expect such calibrations to cause additional subtleties when determining the dark photon energy.

In Fig. 4, we study the $gg \to \Phi(750) \to 2\gamma'$ process and show the required resonance production with the 5 fb diphoton signal at 13 TeV in ATLAS. As expected, changing kinetic mixing affects the event selection acceptance, and the total production cross section needs to be modified accordingly in order to give the 5 fb signal rate in the diphoton channel. Such a signal rate can easily be obtained by a generic choice of the parameter space.

If the dark photon decays after the ECAL, there is a good chance for the signals to be either unconstructible (gives missing energy) or identified as displaced lepton jets [30].

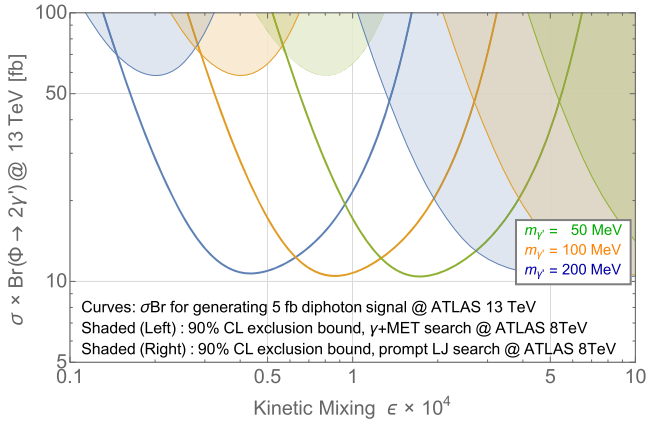

FIG. 4. The required cross section times branching ratio of the scalar resonance $\Phi(750) \to 2\gamma'$ that generates a 5 fb diphoton signal at the 13 TeV ATLAS search, assuming $\mathrm{Br}(\gamma' \to e^+e^-) = 1$. Different color schemes represent various dark photon masses $m_{\gamma'}$, and the shaded regions give the 90% C.L. exclusion bounds from the 8 TeV ATLAS search of a photon + MET [28] (exclusion regions on the left) and prompt lepton jets [25] (exclusion regions on the right). Here we carry out the analysis conservatively by assuming the highly collimated e^+e^- from the light γ' decays cannot be reconstructed if the decay happens after the first layer of the ECAL ($\lesssim$1590 mm). Since the MET in [28] is defined as the imbalance of the total p_T of the constructed objects, we treat such displaced decay as missing energy. When the decay happens before the pixel ($\lesssim$34 mm), the highly collimated lepton pairs are identified as lepton jets. The rescaling of the resonance production between 13/8 TeV is based on the $gg \to \Phi(750)$.

As we discuss in Sec. II, searches of displaced lepton jets do not yet provide relevant constraints. In the monophoton search [28], the MET is defined as the imbalance of the total p_T of constructed objects. If we take the conservative assumption by identifying the decays after the first layer of the ECAL to be contributions to MET, the monophoton search can be applied to constrain the parameter space [28,44]. In Fig. 4, the shaded region on the top left is given by the 90% C.L., exclusion from the monophoton search at the 8 TeV search in [28]. Here we adapt cuts used in the ATLAS search, i.e., requiring one of the dark photons to have $p_T > 150$ GeV, $|\eta| < 1.37$, and decays inside the photon identification region, while the other photon decays after the first layer of the ECAL. The bounds are barely relevant for the parameter space which gives the 5 fb signal rate in the diphoton channel.

If dark photons decay before the first layer of the pixel ($r \lesssim 34$ mm) in the tracker, then such a highly collimated e^+e^- from the dark photon decay can be identified as a lepton jet. ATLAS carries out a search on a prompt lepton-jet pair [25]. This search can be applied to constrain our scenario since it is possible that both dark photons decay before getting into the tracker, especially when the mixing ϵ is large. We show the existing bound on the cross section in the shaded region at the right side of Fig. 4. Lepton jets are required to have $p_T > 5$ GeV, $|\eta| < 2.5$, and we apply a reconstruction factor of 0.6 for each of the jets, which is comparable to the value used in [25]. As we see, the bound is relevant only when the mixing is large and is not useful to constrain most of the interesting parameter space.

It is interesting to study the angular distribution of the fake photons. When the decay length in the lab frame is comparable to the detector size, the geometry of the tracker and ECAL affects the photon faking probability and introduces detector effects to the angular distribution of the signals. The current diphoton analysis in ATLAS imposes hard p_T^γ cuts in the event selections, which remove the decays close to the beam direction. However, a wider range of the angular distribution is necessary for studying the spin of the heavy resonance, and it is useful to relax the p_T^γ cut. When studying the angular distribution in Figs. 5 and 6, we impose the p_T cut in a milder way by requiring $p_T^\gamma > 50$ GeV for both photons.

In Figs. 5 and 6, we take the events that are registered as diphoton under the relaxed p_T cuts. We boost the events

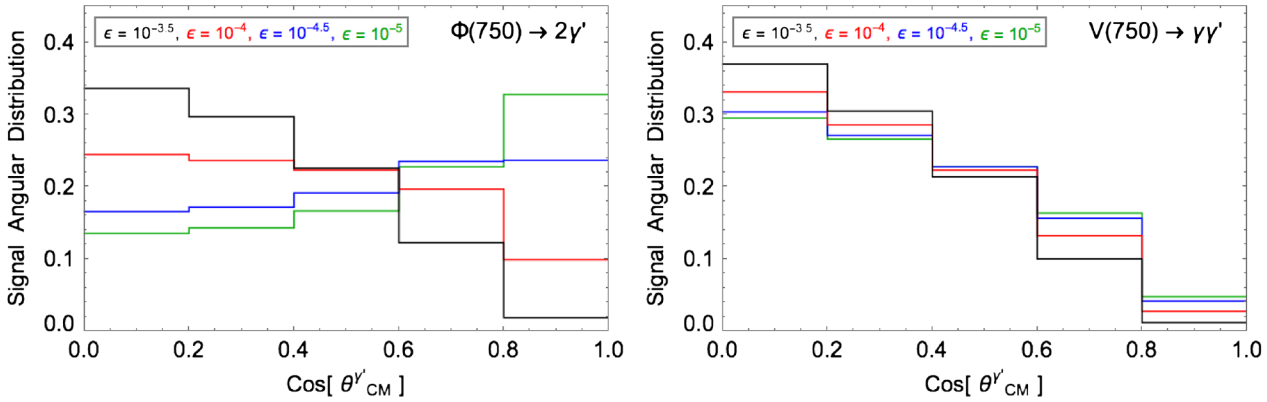

FIG. 5. Here we take the events that pass a mild diphoton p_T cut, as discussed in context. We show the angular distribution of the decay products in the rest frame of the heavy resonance, for scalar (left) and vector (right). Different colors correspond to various choices of ϵ. We take $m_{\gamma'} = 100$ MeV as our benchmark.

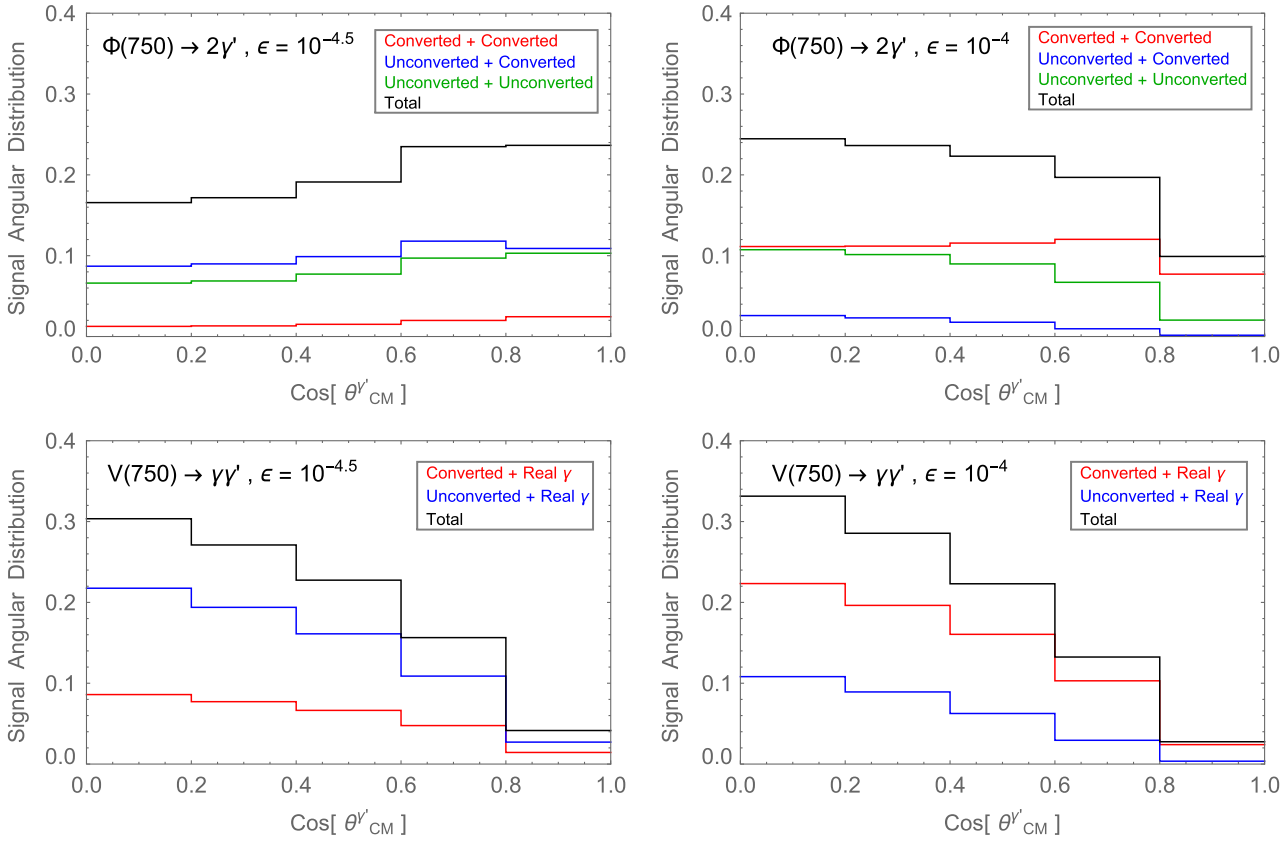

FIG. 6. The angular distribution of the decay products in the rest frame of the heavy resonance, assuming $m_{\gamma'} = 100$ MeV. Different colors specify various categories of photon identification, and the different angular distributions of the signal may provide a handle to distinguish the real and fake photon events. When generating the $V \to \gamma\gamma'$ events, we assume the process is dominated by the transverse component of the massive vectors V and γ'. Note, the scalar decay is a flat distribution in the rest frame before taking into consideration the angular dependent acceptance from the detector. The spin of the vector resonance has a large probability to point along to the beam direction. Thus the vector bosons in the final states are more concentrated in the central region in the rest frame, i.e., smaller $\cos(\theta^{\gamma'}_{\mathrm{CM}})$.

back to the rest frame of the heavy resonance and study the angular distribution of the decay. For both the scalar and vector resonances, the signal becomes more forward when the dark photon has a longer decay length. A larger distance between the interaction point and the ECAL gives the dark photon a greater chance to decay in the right region.

The angular distribution is the way to determine the spin of a particle. In our scenario, the detector effect can easily introduce a bias to the final state distribution, which could cause confusion or even mistakes when studying the spin of heavy resonance without bearing the subtlety in mind. Furthermore, as shown in Fig. 6, angular distribution of various categories of photon identification can be different. This may provide a unique way to distinguish a real photon from the displaced dark photon decay.

VI. DISCUSSION

Object identification in high energy colliders is subtle. In this paper, we study the possibility of faking photon signals at the LHC using displaced decays of the dark photon into e^+e^-. Under a generic choice of parameters, dark photons have a large chance to be identified as a SM photon in detectors. Especially, the decay of a dark photon cannot fake only a converted but also an unconverted photon.

When a dark photon decays at a different region of the detector, it will be identified as a different object according to the object reconstruction strategies. This introduces a detector structure dependence into object identification. More explicitly, given a fixed decay distance, a dark photon propagating along a different angular direction may decay at a different part of the detector, before the tracker, within the tracker, within the ECAL, or outside the ECAL. Thus this dark photon decay can be identified as different objects, such as a lepton jet, a converted photon, an unconverted photon, or even missing energy. The nontrivial angular dependence in the signal efficiency that is generated by the detector structure will further affect the event selection. This can change the result of spin determination of the heavy resonance. More interestingly, since the event selection is sensitive to detailed structures of a detector, the probabilities of faking a photon can be different between ATLAS and CMS. Without unfolding the detector effects, ATLAS and CMS may observe different numbers of fake

photon events. Comparing the signal cross section or the angular distribution between these two experiments may provide a useful and novel handle to distinguish our scenario from conventional ones.

A dark photon that decays within the tracker can fake a real photon. However, that implies a non-negligible probability for the decay to be before or after the tracker. If it decays before the tracker, such an object may be identified as a lepton jet. Further if the decay happens after the ECAL, it can be identified as different objects depending on the detailed decay location. If the decay happens inside the HCAL, it may be identified as a jet with no electromagnetic (EM) energy. Such exotic objects have already been covered in some searches [29,30]. Future improvements, such as triggering on one hard photon and one jet with no EM energy, can be applied in order to increase the sensitivity. If the decay happens in the muon chamber, another specialized displace signal search can be imposed to cover the scenario. Besides to ATLAS and CMS experiments, other dark photon searches can also provide complementary constraints to similar regions of dark photon parameters. For instance, a dark photon with $\mathcal{O}(100)$ MeV mass and $\mathcal{O}(10^{-4})$ mixing can easily fake a SM photon in the benchmark model in this paper. In the meantime, the dark photon search at the LHCb [45] can cover a similar parameter region. However, we note that our dark photon production is based on the decay of a heavy resonance. While in [45] and most of other dark photon searches, the production is only through kinetic mixing. Depending on the production rate of this heavy resonance, we may or may not have an earlier coverage on the similar dark photon parameter region. However, let us emphasize that constraining dark photon parameter space is not our key focus. The goal of this paper is to point out the subtleties in particle identification strategies and study their potential impacts when extracting physics information in certain searches.

Besides the exotic object search, there could be other ways to distinguish the dark photon scenario from other possibilities. In most models where the photons are directly produced from a heavy resonance decay, other diboson channels such as $Z\gamma$ and ZZ have non-negligible rates. This is because the particles mediating the diphoton decay channel also couple to the Z boson. However, this relation does not necessarily hold if the heavy resonance decays dominantly to two dark photons. The decay branching ratios to channels with one or two Z bosons can be highly suppressed by powers of ϵ's from the kinetic mixing. Comparing other diboson decay channels with the diphoton channel then serves as a powerful probe to distinguish models where photons are directly produced from heavy resonance decay or faked by metastable particle decays.

Although in this paper we focus on heavy resonance decaying into dark photons, our study really highlights the possibility of faking photons using dark photon decays. The lesson one can draw here has a much broader implication. Dark photons can provide alternative interpretations of many searches of new physics with photon(s) in the final state. On the other hand, when searching dark photons, we may also miss the signal by mistagging the displaced dark photon decay as a regular photon. It is important to explore such possibilities and develop more sophisticated strategies to distinguish these fake objects.

ACKNOWLEDGMENTS

We are grateful to Alberto Belloni, David Curtin, Michael Mulhearn, Myeonghun Park, and Haichen Wang for useful discussions. Y. T. is supported by the National Science Foundation Grant No. PHY-1315155, and by the Maryland Center for Fundamental Physics. L. T. W. is supported by DOE Grant No. DE-SC0013642. Y. Z. is supported by DOE Grant No. DE-SC0007859.

[1] B. A. Dobrescu, G. L. Landsberg, and K. T. Matchev, Phys. Rev. D **63**, 075003 (2001).
[2] S. Chang, P. J. Fox, and N. Weiner, Phys. Rev. Lett. **98**, 111802 (2007).
[3] F. Larios, G. Tavares-Velasco, and C. P. Yuan, Phys. Rev. D **64**, 055004 (2001).
[4] F. Larios, G. Tavares-Velasco, and C. P. Yuan, Phys. Rev. D **66**, 075006 (2002).
[5] N. Toro and I. Yavin, Phys. Rev. D **86**, 055005 (2012).
[6] P. Draper and D. McKeen, Phys. Rev. D **85**, 115023 (2012).
[7] S. D. Ellis, T. S. Roy, and J. Scholtz, Phys. Rev. Lett. **110**, 122003 (2013).
[8] S. D. Ellis, T. S. Roy, and J. Scholtz, Phys. Rev. D **87**, 014015 (2013).
[9] D. Curtin *et al.*, Phys. Rev. D **90**, 075004 (2014).
[10] J. Chang, K. Cheung, and C.-T. Lu, Phys. Rev. D **93**, 075013 (2016).
[11] L. Aparicio, A. Azatov, E. Hardy, and A. Romanino, J. High Energy Phys. 05 (2016) 077.
[12] S. Knapen, T. Melia, M. Papucci, and K. Zurek, Phys. Rev. D **93**, 075020 (2016).
[13] P. Agrawal, J. Fan, B. Heidenreich, M. Reece, and M. Strassler, J. High Energy Phys. 06 (2016) 082.
[14] B. Dasgupta, J. Kopp, and P. Schwaller, Eur. Phys. J. C **76**, 277 (2016).
[15] Note, the fact that both converted and unconverted photons can be faked by a metastable light particle decaying to $e+/e-$ was also pointed out in [16,17]. However, we take

a different choice of borderline to divide a converted photon versus an unconverted photon. The difference comes from whether stand-alone TRT tracks can be used to distinguish converted and unconverted photons. It is important to notice that the reconstruction efficiency of the track by TRT decreases when increasing p_T, as shown in Fig. 6 on p. 119 of [18]. Since we are mainly focused on the high energy regime of the diphoton resonance search, we expect TRT track reconstruction efficiency is very low and thus negligible. This is one of the crucial differences in our study.

[16] X.-J. Bi, Z. Kang, P. Ko, J. Li, and T. Li, arXiv:1602.08816.

[17] C.-Y. Chen, M. Lefebvre, M. Pospelov, and Y.-M. Zhong, J. High Energy Phys. 07 (2016) 063.

[18] G. Aad *et al.* (ATLAS Collaboration), arXiv:0901.0512.

[19] G. Aad *et al.* (ATLAS Collaboration), J. Instrum. **3**, S08003 (2008).

[20] CERN Technical Report No. ATLAS-CONF-2012-123, 2012.

[21] This is only a requirement on seeding a track candidate. A more stringent and complicated analysis will be carried out in order to reconstruct a track. In the following discussion, we will assume all tracks can be reconstructed once they are seeded. This will introduce a bias that enlarges the probability of identifying our metastable particle decay as a converted photon instead of a normal photon, as discussed in later context.

[22] The ATLAS Collaboration, CERN, Technical Report No. ATLAS-CONF-2016-059, 2016.

[23] V. Khachatryan *et al.* (CMS Collaboration), Phys. Rev. Lett. **117**, 051802 (2016).

[24] S. Gonzi, CERN Technical Report No. CMS-TS-2014-008, 2014.

[25] G. Aad *et al.* (ATLAS and CMS Collaborations), J. High Energy Phys. 02 (2016) 062.

[26] This particular definition of MET is widely used in many other searches involving missing energy. See also [27] for the MET reconstruction at CMS. The benefit for doing this is because, for a well-reconstructed object, its transverse momentum can be properly calibrated according to its identity. However, if an object is not well defined in a particle-flow event reconstruction, such as a dark photon decaying after ECAL, this object is unlikely to be included when calculating MET.

[27] CMS Collaboration, Technical Report No. CMS-PAS-PFT-09-001, 2009.

[28] G. Aad *et al.* (ATLAS Collaboration), Phys. Rev. D **91**, 012008 (2015); **92**, 059903(E) (2015).

[29] ATLAS Collaboration, CERN Technical Report No. ATLAS-CONF-2014-041, 2014.

[30] G. Aad *et al.* (ATLAS Collaboration), J. High Energy Phys. 11 (2014) 088.

[31] ATLAS Collaboration, CERN Technical Report No. ATLAS-CONF-2015-081, 2015.

[32] CMS Collaboration, CERN Technical Report No. CMS-PAS-EXO-15-004, 2015.

[33] This is the case if the dark photon couples to the 750 GeV heavy resonance through a triangle loop induced by heavy fermions. The longitudinal mode is suppressed by the small Yukawa coupling between a dark Higgs and a heavy charged particle running in the loop.

[34] The angular distribution of a transversely produced dark photon decay is $\frac{d\mathrm{Prob}(\theta)}{d\cos\theta} \propto (1+\cos\theta^2)$ in the center-of-mass frame, where θ is the open angle between e^- and the spin direction. Here we assume the resonance mass $\gg m_{\gamma'} \gg m_e$, and the obtained energy ratio distribution is $\frac{d\sigma}{dx} \propto (1-\frac{2x}{(1+x)^2})/(1+x)^2$, with $x \equiv E_{\mathrm{Soft}}/E_{\mathrm{Hard}}$ in the lab frame.

[35] http://www.physics.smu.edu/~web/research/preprints/SMU-HEP-08-13.pdf.

[36] This is the average width of a strip cell. The precise number is angular dependent due to detector details, and we take only one fixed number in our analysis to simplify the calculation. The result from this estimation should only be different from the real answer by a factor of O(1).

[37] M. Chala, M. Duerr, F. Kahlhoefer, and K. Schmidt-Hoberg, Phys. Lett. B **755**, 145 (2016).

[38] See [39] for more discussions on the bound state production with self-interacting dark matter coupled through dark photons and [16] for the discussion of asymmetric dark matter. Also see [40] for having the 750 GeV resonance as a bound state of heavy colored fermions.

[39] Y. Tsai, L.-T. Wang, and Y. Zhao, Phys. Rev. D **93**, 035024 (2016).

[40] C. Han, K. Ichikawa, S. Matsumoto, M. M. Nojiri, and M. Takeuchi, J. High Energy Phys. 04 (2016) 159.

[41] J. Alwall, R. Frederix, S. Frixione, V. Hirschi, F. Maltoni, O. Mattelaer, H. S. Shao, T. Stelzer, P. Torrielli, and M. Zaro, J. High Energy Phys. 07 (2014) 079.

[42] A. Alloul, N. D. Christensen, C. Degrande, C. Duhr, and B. Fuks, Comput. Phys. Commun. **185**, 2250 (2014).

[43] G. Aad *et al.* (ATLAS Collaboration), Eur. Phys. J. C **74**, 3071 (2014).

[44] V. Khachatryan *et al.* (CMS Collaboration), Phys. Lett. B **750**, 494 (2015).

[45] P. Ilten, J. Thaler, M. Williams, and W. Xue, Phys. Rev. D **92**, 115017 (2015).